# Modelling of flow and heat transfer, mixing and morphology development in plasticating single screw extrusion of polymer systems

José A. Covas, A Gaspar-Cunha

Dept. Polymer Engineering/Institute for Polymer and Composites

University of Minho, Guimarães, PORTUGAL

**Abstract**

Models for flow and heat transfer, morphology development of liquid-liquid and solids-liquid systems and mixing assessment in conventional single screw estruders are introduced. Their computer implementation and interdependence are explained. Representative predictions are discussed with the aim of illustrating the capability of these models as wells as showing the typical response of single screw extruders.

## 1. Introduction

Single screw extruders are a crucial element of the extrusion lines used for the manufacture of plastics products such as tubular and flat films, sheets, pipes & tubing, profiles, wire & cable, mono and multifilaments, fibers, nets, bottles and other hollow containers, etc. Their role is to pump towards the shaping die a homogeneous melt at the highest possible constant rate. To accomplish this, the machine must be able to receive the raw material in powder or granular (the most frequent) form, melt it, homogenize it (both in terms of temperature and composition), and generate the pressure necessary for extrusion at the anticipated rate. The term *plasticating* applied to single screw extrusion designates the sequence of physical phenomena experienced by the polymer from the moment it enters the extruder until it exits the die.

The performance of single screw extruders is determined by the material properties, the geometrical/constructive features of the machine and the operating conditions selected (usually, screw speed and axial temperature profile). If a specific process behavior could be predicted rather than determined experimentally (this usually involves a significant number of expensive and time consuming trial and error attempts), better screw designs, higher quality products and greater outputs could be achieved faster and cheaper. Therefore, not surprisingly,

plasticating single screw extrusion has been extensively studied both in academia and industry. Initially (between the 1950s and the 1960s), efforts were made to understand the physical phenomena developing along the screw. Various attempts to model (parts of) the process were also published (between the 1960s and 1980s) [1-6]. Later, a number of overall models of plasticating extrusion were progressively made available as commercial software packages. The present chapter presents an overall model of plasticating extrusion that was conceived to balance completeness and precision of the predictions with reasonable computational costs. In turn, this model was subsquently coupled to other algorithms that yield supplementary data about the process. One example is process optimization, which will be dealt with in a separate chapter.

Moreover, although models of plasticating extrusion assume the presence of a specific homopolymer, currently more complex material systems are processed, such as compounds comprising polymers and specialized additives, polymer blends, polymer composites and nanocomposites. In most cases, upon melting and subsequently downstream, a multiphase liquid–liquid or liquid-solid morphology develops. It is well accepted that the final morphology determines the performance of the material under service conditions. Therefore, it is important to predict the progress of the morphology of liquid–liquid or solid-liquid systems during plasticating extrusion. This can be done by implementing a morphology development model and coupling it to a plasticating model, which will deliver information on local flow conditions (velocities, temperatures and residence times). Morphology development models for liquid-liquid and solid-liquid systems will be presented in this chapter. Finally, the data supplied by such models can be used to assess the mixing capability of a particular extruder, both in terms of distributive and dispersive mixing.

The present chapter is structured in three main parts. First, models for flow and heat transfer (i.e. plasticating), morphology development and mixing assessment are introduced. They are preceded by a presentation of the geometry assumed for the calculations. The second part explains the computer implementation of the above models. In general, this involves coupling the routine for flow and heat transfer to one of the other algorithms. Finally, the third part discusses some representative results.

## 2. Modelling the process

### 2.1 Geometry

Figure 1 illustrates the typical layout of a standard single-screw extruder. It consists essentially of a hollow long barrel (with a length to diameter ratio, L/D, typically equal to or above 24), inside which one Archimedes-type screw rotates at a controllable constant speed (the machine comprises also a DC or AC drive motor, a speed reducing gear and a control panel, which are not represented in the figure). A shaping die is coupled to one end of the barrel, while the raw material is fed by a lateral hole at the opposite end (commonly known as feed throat), on top of which a hopper is fixed. The latter usually consists of a vertical column with straight and/or inclined sections and contains the raw material to be processed, usually in pellet form. The screw shown in the Figure 1 has a constant pitch and a variable channel depth, thus producing three geometrically distinct zones. From hopper to die, one can identify a feed zone (with constant channel depth), a compression zone (with decreasing channel depth) and a metering zone (where the screw is shallower). Heater bands surround the barrel and die. Together with thermocouples and temperature controllers, they allow to set and maintain a specific axial temperature profile. At constant geometry, changing the set temperatures and/or the screw speed, will create distinct thermomechanical environments inside the machine.

The flow channel linking the feed throat to the die (i.e., the free volume inside the barrel to be occupied by polymer) is helical, with the pitch of the screw, an approximately rectangular cross-section, and a depth that is either constant or gradually decreasing, depending on the lengthwise location. Therefore, the simplest straight progress of a pellet or fluid element along this channel is mathematically described by the equation of helix, if a Cartesian coordinate system, for example with its origin positioned at the start of the extruder is assumed. If the flow is more complex, equations will become inevitably also more complicated. This difficulty originated three classic assumptions that are habitually adopted when modelling single screw extrusion. One concerns the cinematics, two refer to the geometry of the system:

a) Although the screw rotates inside a motionless barrel, the opposite is assumed, i.e., the screw is considered as stationary, and the barrel is assumed to rotate in the opposite direction at the same angular velocity;
b) The helical channel and the barrel are considered as unwrapped. In other words, the helical channel becomes a rectangular channel whose lateral walls are the pushing and trailing flights of the screw, and the bottom is the screw root (in reality, the helical geometry causes the helix angle to depend on radius, but the distortion caused upon unwrapping is disregarded). The depth changes along the length, as seen above.

Likewise, the barrel becomes a flat surface sliding on top of the rectangular screw channel towards the die. Considering assumption a), this sliding motion makes an angle relative to the channel, which is the screw helix angle;

c) Given a) and b), the Cartesian coordinate system can now be attached to the stationary screw channel; axes *x,y,z* correspond to directions across the channel, upwards and along the channel, respectively.

As a result of these assumptions, a movement of material straight along the channel is now simply described by the equation of a straight line. These assumptions are thus quite convenient and will be adopted in this chapter.

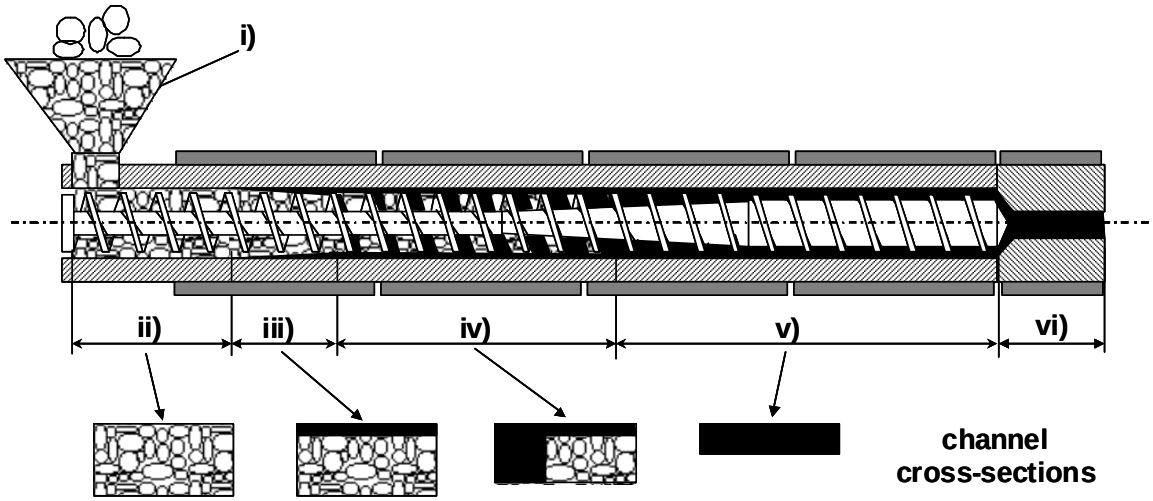


Figure 1- Geometrical layout of a single screw extruder and plasticating sequence; the pellets are stored in the hopper and fed through a lateral opening in the barrel; they advance along the screw and are progressively melted, the melt exists the die at the opposite end; (i) to vi) represent process stages identified in the text).

### 2.2 Modelling flow and heat transfer

To model the plasticating process of the polymer inside a single screw extruder, it is first necessary to identify the physical phenomena developing from the instant the material enters the channel until it emerges from the die. These are schematically illustrated in Figure 1. The pellets enter the channel via the hopper by gravity-induced flow. Then, the material is dragged along the screw due to friction (it slides along the screw due to the friction created by the inner barrel surface) until it melts. Melting is initiated near to the inner barrel surface due to the

combined effect of heat conduction from the barrel and mechanical energy dissipation due to the friction forces. Melting of the bulk solids develops gradually following a well-ordered mechanism that involves the segregation of the melt from the surviving solids. Due to the relative barrel-screw movement, the melt formed near to the inner barrel wall accumulates in a melt pool that co-exists side by side with the solid bed. The width of the former increases progressively along the channel, while that of the latter reduces, until all the material is molten. In the last portion of the screw, the melt advances following a helical pattern, generating pressure and some degree of distributive mixing, until it flows through the die taking approximately the desired shape. Extensive experimental research demonstrated that this sequence of phenomena is quite general, although the rate of development and the extent of each stage are affected by the operating conditions, material properties and channel geometry. Consequently, as shown in Figures 1 and 2, plasticating extrusion can be taken as the sequence of the following individual stages (also known as functional zones):

i) gravity-induced *solids conveying* in the hopper;

ii) *drag solids conveying* in the initial screw turns;

iii) *delay in melting*, due to the growth of a thin melt film between the solids and the channel wall(s);

iv) *melting* according to a specific mechanism;

v) *melt conveying*, consisting of a helical flow pattern of the fluid towards the die;

vi) *die flow*.

Each of these stages is described mathematically by a set of general equations, together with the relevant constitutive laws and boundary conditions. In turn, all the stages are linked by appropriate boundary conditions, thus yielding a global coherent plasticating model.

The hopper consists of a sequence of vertical and/or divergent columns holding thousands of loose pellets with various shapes, an average particle size, and a particle size distribution. The pellets descend due to gravity, enter the channel of the rotating screw and then progress downstream with a complex velocity profile due to friction with the barrel, with the screw walls and between pellets, due to gravity, and due to particle-particle and particle-wall collisions. The packing density and temperature of the particles increase progressively until the solids form a cohesive elastic solid-plug. The flow of the individual pellets in the hopper and in the initial screw turns can be computed numerically by means of the discrete element method (DEM) [7,

8]. Mass output, volume fraction, average residence time, residence time distribution and velocity profiles (in the cross-channel and down-channel directions) can be predicted, but only after a significant computation effort. In practice, this approach has been used to study solids conveying independently, but has never been linked to the remaining plasticating stages because of the resultant excessive computation times. It has been demonstrated that the free flow capacity of a hopper is much higher than the actual discharge rate verified when it is mounted on top of the feed opening of an extruder [4]. Thus, a static vertical pressure profile may be assumed and calculated using the analysis proposed by Walker [9], which is based on a force balance on an elemental horizontal bulk solids slice. The pressure at the bottom of the hopper represents inlet condition of the sceew channel. Drag solids conveying (see Figure 2) is usually modelled assuming the sliding of a non-isothermal elastic solid plug between two parallel plates (barrel and screw root) with different friction coefficients. The thermal effect results from the contribution of conduction from the hot barrel and of friction near to the polymer/metal interfaces [10, 11]. The pressure generated between the screw inlet and the subsequent process stage is determined from force and torque balances made on differential down-channel elements. Pressure rises exponentially along the channel, the increase being linked to the relative value of the fiction coefficients [12].

A delay zone (delay in melting, Figure 2) is often presumed as developing after drag solids conveying [13]. Indeed, friction and heat transfer will ultimately lead to the melting of the solids near to the inner barrel wall (and later, at the solids/screw interface). A film is then formed. When, due to the relative screw-barrel movement, this molten material can no longer flow backwards through the gap between the barrel and the screw tip, or through the spaces between contiguous pellets, a melt pool is formed near to the active flight and the melting stage initiates [14]. Thus, the delay zone can be sub-divided into two sequential phases. First, a melt film is formed near to the barrel wall (Figure 2, delay in melting-B). In the calculations, the friction force for drag solids conveying is replaced by a shear stress applied by the film on the solid bed. The film thickness and temperature can be obtained by solving the relevant forms of the momentum and energy equations, taking in heat convection in the down-channel and radial directions and heat conduction in the radial direction. In the second phase, films of molten material are created near to the screw channel walls (films B, D and E in Figure 2, delay in melting-B). From a modelling point of view, this can be viewed as a special state of melting, which develops while the width of melt film B remains smaller than the channel height [15].

Tadmor and Klein [1] developed a melting model based on the important experimental observations reported by Maddock [16] in the fifties. Subsequently, several variants were

proposed with the aim of relaxing progressively some of the initial assumptions, and thus make the model more realistic. As illustrated in Figure 2 (melting), Lindt *et al* [17, 18] assumed the existence of the main melt pool (B), of a film (C) separating the barrel and the solid plug (A), and molten films separating the solid plug from the lateral and bottom screw walls (D,E). Constant down-channel solid bed velocity and cross-channel flow recirculation were also postulated. Flow and heat transfer in each of the 5 regions were described by different forms of the momentum and energy equations, coupled to the relevant boundary conditions and force, heat and mass balances [15].

The precise description of the flow of molten polymer during melting and melt conveying requires a full 3D analysis. However, if the overall modeling of the plasticating sequence is to be associated with morphology development and optimization, the necessary computational times would become unreasonable. Thus, melt conveying is often assumed as a two-dimensional non-isothermal flow of a non-Newtonian fluid. Considering that flow is incompressible and both flow and temperature are fully developed in the down and cross-channel directions, and that the viscosity is described by a Carreau-Yasuda law, the mass conservation, momentum and energy equations are solved, coupled to the relevant boundary conditions. Domingues *et al* [19] compared the predictions produced by this approach with those obtained by a 3D analysis using the ANSYS Polyflow® software [20]. The average differences associated with $V_x$, $V_y$, and $V_z$ (the velocities in the x, y, and z directions, respectively) were 10.4%, 2.9%, and 6.5%, respectively, thus supporting the utilization of the simplified approach.

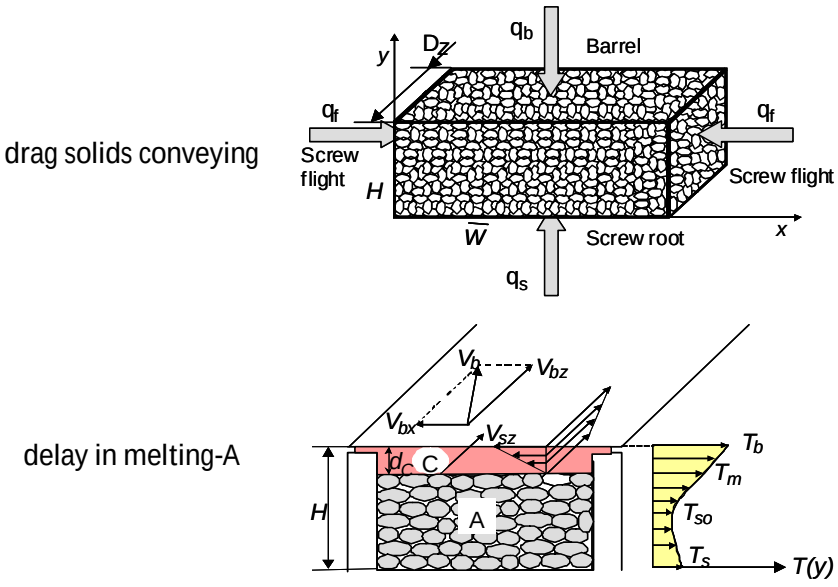

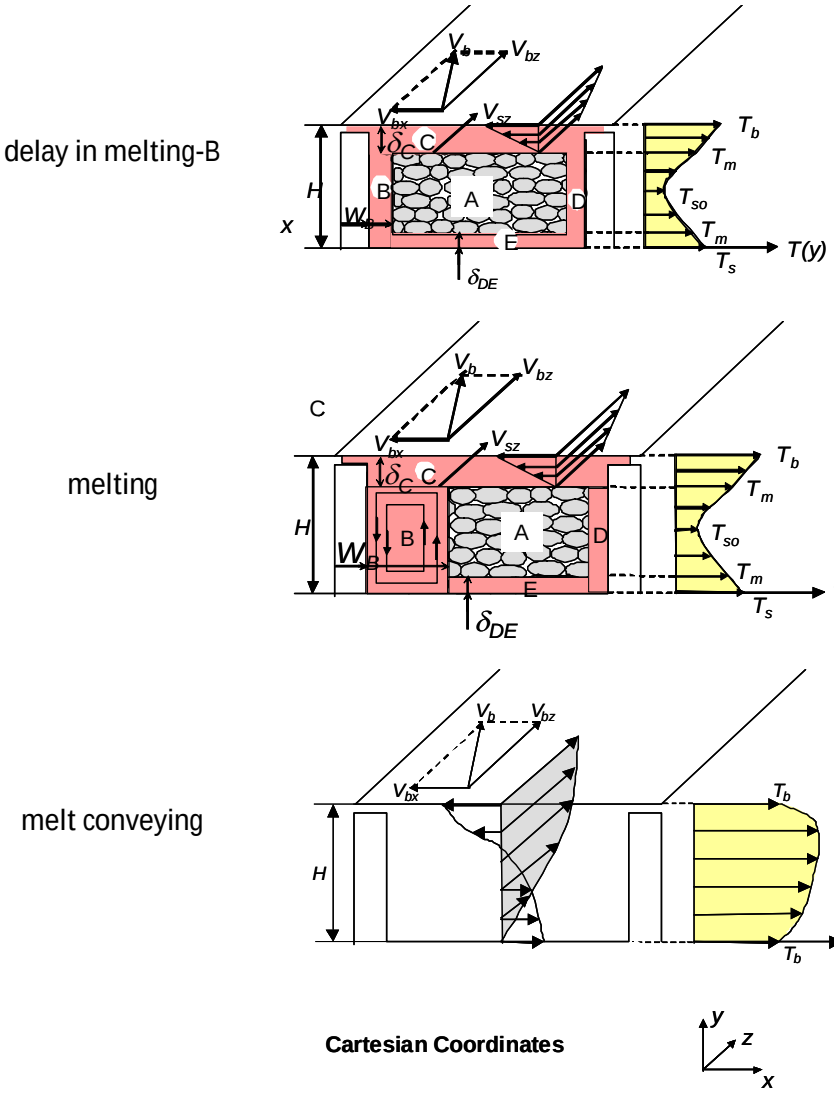


Figure 2- Physical models for the functional zones developing along the screw channel in plasticating single screw extrusion.

### 2.3 Modeling morphology development in liquid-liquid systems

Since the material or materials to be extruded are generally fed as solids in the hopper, a mathematical description of the development of the morphology of a multiphase liquid–liquid system along the screw must encompass the melting and melt conveying zones, and consider the relevant deformation, break-up and coalescence phenomena usually associated to these systems [21]. The break-up and coalescence processes compete against each other, and it is the overall result of this contend that determines the final drop size distribution.

A number of Maddock-type experiments were performed with immiscible and compatibilized Polyamide/Polypropylene blends, under a variety of operating conditions and screw profiles

[22]. The authors reported that the melting stage follows a more complex mechanism than that accepted for homopolymers (and discussed in the previous section). Instead, a competition between a Tadmor-type model involving the co-existence of a melt pool and a solid bed and melting of individual solid pellets suspended in the melt was observed. This is probably related to the fact that the polymers had distinct melting temperatures and rheological properties. Since a melting model for this hybrid sequence is not currently available, melting of the major component (the one with higher concentration) will be assumed, and uniformly distributed suspended drops of the minor component will be inserted [19] at the pace of melting. The morphological model aims at estimating the evolution of the dimensions of these entities along the screw channel.

During flow, the suspended droplets will be subjected to affine deformation due to shear, i.e., they will stretch progressively. For a simple shear flow, the growth in length (L) can be correlated with the shear deformation (γ) and the initial drop diameter (d) through [19]:

$$L = \begin{cases} \left(1 + \frac{\gamma^2}{2} + \frac{\gamma}{2}\sqrt{4+\gamma^2}\right)^{0.5} \cdot d & \text{if} \quad \gamma < 5 \\ \gamma \cdot d & \text{if} \quad \gamma \geq 5 \end{cases} \tag{1}$$

The size of the droplets may be reduced by erosion or break-up. The former consists in the removal of small fragments from the drop surface, but this usually embodies a minor effect and will be disregarded here. Break-up occurs when the viscous forces are sufficiently higher than the interfacial tension and act during enough time. The ratio between the viscous forces (given by $\eta_c * \dot{\gamma} * r$, which represent matrix viscosity, shear rate and drop radius, respectively) and the interfacial tension ($\upsilon_{12}$) is known as the Capillary number (Ca). The Ca required for break-up is usually known as critical Ca (Ca*). The time required for drop break-up ($t_b$) is given by [19]:

$$t_b = \frac{2\eta_c r}{\upsilon_{12}\Omega} Ln\left(\sqrt{\frac{r}{\alpha}}\right); \tag{2}$$

where Ω is a long function [21], λ is an index whose value depends on flow type (it assumes the value of 1 for extensional, 0.5 for shear, and 0 for rotational flow), *p* is the ratio between the

viscosity of the dispersed phase and that of the matrix ($\eta_d/\eta_c$) and $\alpha$ is the amplitude of the initial deformation. Grace [23] established a well-known correlation between Ca* and *p* for a spherical drop suspended in a homogeneous steady flow. When Ca > 2 Ca*, the initial droplet deforms extensively and bursts into numerous smaller droplets; when Ca*< Ca < 2 Ca*, the droplet is expected to break into two equal spherical droplets [24]. In the case of low Reynolds numbers, a third smaller droplet can also be created and reportedly has a volume of 10–17% of that of the initial droplet [25].

When two drops collide and move jointly in a shear flow during enough time, coalescence may take place, i.e., the droplets can merge into a single larger entity. For calculation purposes, two successive steps of the process are assumed: (i) the collision of two equal drops and (ii) the exclusion of the polymer film separating them, which will flow into the main stream. The coalescence probability ($P_{coal}$) can be defined as the product of the probability of the two drops colliding ($P_{coal}$), with the probability of film exclusion between the drops ($P_{exc}$) [26]:

$$Pcoal = \exp\left( -\frac{\pi}{8\,\dot{\gamma}\,\phi\,t_{loc}} \right) \tag{3}$$

$$P_{exp} = \exp\left[ -\frac{\sqrt{3}}{4}\left( \frac{r}{h} \right) p.Ca^{3/2} \right] \tag{4}$$

Equation (4) is valid for p~1. Φ is the volume fraction of the dispersed phase, $t_{loc}$ is the local residence time and *h* is the critical value at which the liquid film breaks.

The phenomena taken into consideration along this section must be interrelated with a proper description of the flow developing along the extrusion screw, since information on the onset and length of the melting zone, velocities, temperatures and residence times are necessary to predict the morphology development.

### 2.4 Modelling agglomerate dispersion in solid-liquid systems

The solid particles added to polymers upon processing (e.g., fillers, fibers) usually consist of agglomerates with a hierarchical structure: agglomerates are clusters of aggregates, and these contain numerous primary particles. Cohesive forces hold these structures together.

Consequently, the dispersion of these assemblies can only occur when the hydrodynamic stresses developed during flow along the screw ($\sigma_m$) overcome their cohesive strength ($\sigma_c$). Dispersion can take place through erosion (small fragments detach from the outer surface of the agglomerate) and/or rupture (the agglomerate fragments into aggregates). In principle, the critical stress for erosion is smaller than that required for rupture, but erosion is a much slower process. Based on these concepts, Manas-Zloczower and co-workers [27] proposed the concept of a fragmentation number (Fa), defined as the ratio $\sigma_m/\sigma_c$, and suggested (for silica agglomerates of various densities suspended in low molecular weight polymers) that erosion takes place when $2 \leq Fa < 5$, while rupture occurs rapidly when $Fa \geq 5$. These limits will be adopted here, due to the lack of experimental data on the cohesive strength of most agglomerates used in polymer processing (including calcium carbonate, titanium dioxide, carbon black, carbon nanotubes, organoclays, exfoliated graphite, etc).

Even at high Fa, there is a finite probability associated with the break-up of agglomerates, which is defined as $P_{break} = \lambda^*\Delta t$, with $\lambda^*\Delta t << 1$, where $\lambda$ is a probability per unit time, proportional to the surface area of the agglomerate. The time interval $\Delta t$ is set as a function of screw speed [28]:

$$\Delta t = \frac{kH}{\pi N D_b} \tag{5}$$

$P_{break}$ increases with increasing residence time and agglomerate size. There is an obvious parallelism between Fa and $P_{break}$ and Ca and $t_b$ (see previous section) for liquid-liquid systems.

This dispersion model must be coupled to a numerical model of plasticating extrusion and applied to the melting and melt conveying zones. As in the procedure developed for liquid-liquid systems, a number of initial agglomerates are inserted in the melt pool proportionally to the rate of melting. At the end of melting, the total number of inserted agglomerates corresponds to the filler concentration in the system. The dynamics of particle size distribution are calculated from the location where fillers are inserted until the screw tip.

### 2.5 Assessing mixing

Mixing, i.e., the reduction of spatial composition non-uniformity, is generally an important process pre-requisite for optimal product performance. It can be achieved through two routes. The spatial arrangement of the formulation components can be improved by imposing a certain

shear deformation history, this being known as distributive mixing. The latter depends on the interfacial area generated, which is proportional to the applied strain (defined as the product of shear rate and residence time). Thus, knowing the velocity field, it is possible to map the total strain for the various fluid elements in the screw channel. This was done, for example, by Pinto and Tadmor [29], who computed the degree of distributive mixing during melt conveying using a weighted-average total strain (WATS), assuming isothermal Newtonian flow between parallel plates. A review of other mixing calculation approaches can be seen in [5,6,21]. Composition non-uniformity can also be improved by decreasing the size of at least one of the components of the formulation (for example, droplets of the minor phase for an immiscible polymer blend, or solid agglomerates in the case of a filled system, as discussed above). This means that the computation of dispersive mixing in single screw extrusion requires the complete identification of the size, shape, orientation, and spatial location of every particle or droplet of the minor component along the flow channel. In this section, general mixing indices are proposed to quantify the degree of distributive and dispersive mixing in single-screw extruders. They are obtained by coupling a description of the flow in the screw from hopper to die to the models of morphology evolution previously discussed. Thus, processing of liquid-liquid and solid-liquid systems are dealt with individually.

In the case of liquid-liquid systems, the degree of distributive mixing can be estimated using the concept of striation thickness [6,21]. As seen previously, during the affine deformation of a droplet subjected to a simple shear flow, its length increases gradually as described by equation (1). A similar expression can be derived for the width of the drop, B [21,28]. In these equations, the drop diameter (d) changes if the drop breaks. Therefore, if $d_i$ is the initial drop diameter, $B/d_i$ represents the width reduction. The degree of distributive mixing may be quantified by [28]:

$$mix_{dist} = \frac{\sum_{j}^{N}\left[\left(\frac{d}{d_i}\right)_j \times \left(1-\frac{B}{d_i}\right)_j\right]}{\sum_{j}^{N}\left(\frac{d}{d_i}\right)_j} \tag{6}$$

where $N$ is the total number of drops. Similarly, the degree of dispersive mixing can be defined as:

$$mix_{disp} = \frac{\sum_{j}^{N}\left[\left(\frac{d}{d_i}\right)_j \times \left(1-\frac{d}{d_i}\right)_j\right]}{\sum_{j}^{N}\left(\frac{d}{d_i}\right)_j} \tag{7}$$

For solid-liquid systems, distributive mixing can be measured using an entropic measure, such as the Shannon entropy, as proposed by Manas-Zloczower and co-workers [27]. Dividing the system in *M* equal sub-regions, the Shannon entropy can be calculated from:

$$S = -\sum_{j=1}^{M} p_j \log p_j \tag{8}$$

where $p_j$ is the probability of finding a particle in sub-region *j*. The Shannon entropy is maximized when the probability of finding a particle in each sub-region is the same and is nil when all the particles are located in a single sub-region. A Shannon entropy normalized to its maximum value can be used as a distributive mixing index:

$$mix_{dist} = \frac{-\sum_{j=1}^{M} p_j \, log \, p_j}{log(M)} \tag{9}$$

The global degree of dispersive mixing can be estimated from Eq. (7), where *d* now represents the diameter of the solid agglomerates.

## 3. Computer Implementation

As seen above, the global plasticating extrusion model describing flow and heat transfer between hopper and die must encompass a number of individual stages that are linked sequentially through appropriate boundary conditions. Output is one of the unknowns of the problem. Therefore, as seen in Figure 3, before proceeding with calculations along small down-channel screw increments, an initial output is guessed from volumetric considerations. During the calculations, the local development of solids conveying, melting, or melt conveying is detected and velocity and temperature profiles ate computed. Once the calculations are

completed, if the predicted pressure drop at the die exit is not sufficiently small (theoretically, it should be nil), the output is changed and a new iteration is performed, the process being repeated while necessary. The results obtained include global process parameters, such as mass output, mechanical power consumption, axial length of screw required for melting, average melt temperature, degree of distributive mixing (WATS) and maximum viscous dissipation (ratio of maximum melt temperature to local barrel temperature), as well as the progress along the screw of a few variables, like solids and melt pressure, relative presence of solids, melt temperature, and mechanical power consumption.

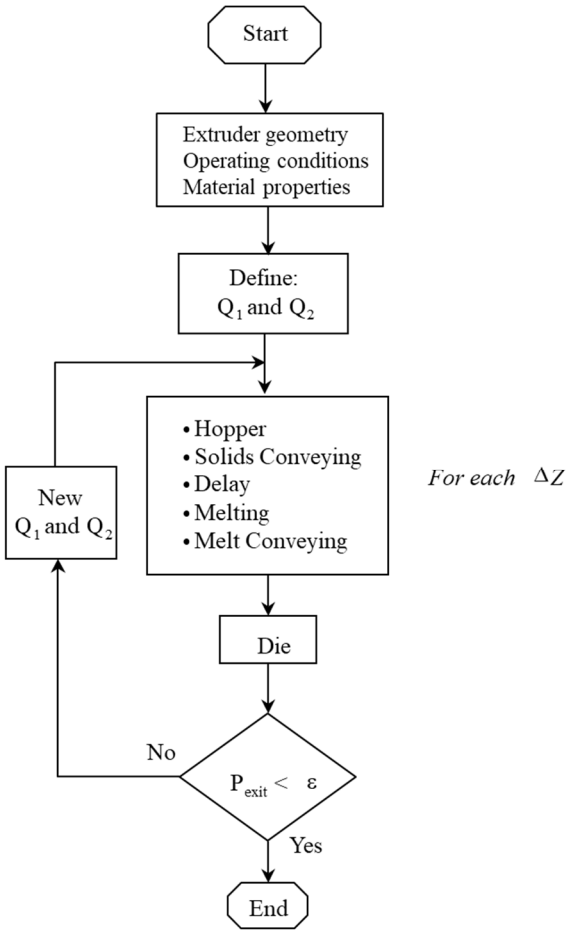


Figure 3- Flowchart for modelling flow and heat transfer along the screw.

The evolution of the morphology for liquid-liquid or solids-liquid systems, as well as the estimation of the resulting degree of distributive and/or dispersive mixing involves an interrelation with the description of flow and temperature tackled above. Figures 4 and 5 depict the corresponding flowcharts. For liquid-liquid structures, the main steps are the following (figure 4):

a) Compute velocity and temperature profiles in the screw channel;

b) Compute the local viscous forces and compare the maximum with the interfacial tension of the minor component; if it is high enough, the time for breakup is calculated;

c) Compare the local residence time with the breakup time; if break-up occurs, the droplet is replaced by smaller spherical ones;

d) Test for coalescence probability - if it is likely, set the new drop dimensions;

e) If the drop does not break nor coalesce, calculate its new width;

f) Repeat the calculations in the remaining fractions of the same channel cross section;

g) Evaluate the mixing indices for the channel cross-section under consideration;

h) Repeat the above steps for a downchannel increment, until reaching the outlet.

For solid-liquid systems, the sequence of calculations is (figure 5):

a) Compute velocity and temperature profiles in the screw channel;

b) Apply a Monte Carlo scheme to determine a breakup probability, which is then compared with a random number in the interval [0,1]; if it is higher, breakup can occur;

c) Compute the fragmentation number and set the dispersion mode;

d) Estimate new particle dimensions;

e) Same as steps f) to h) above.

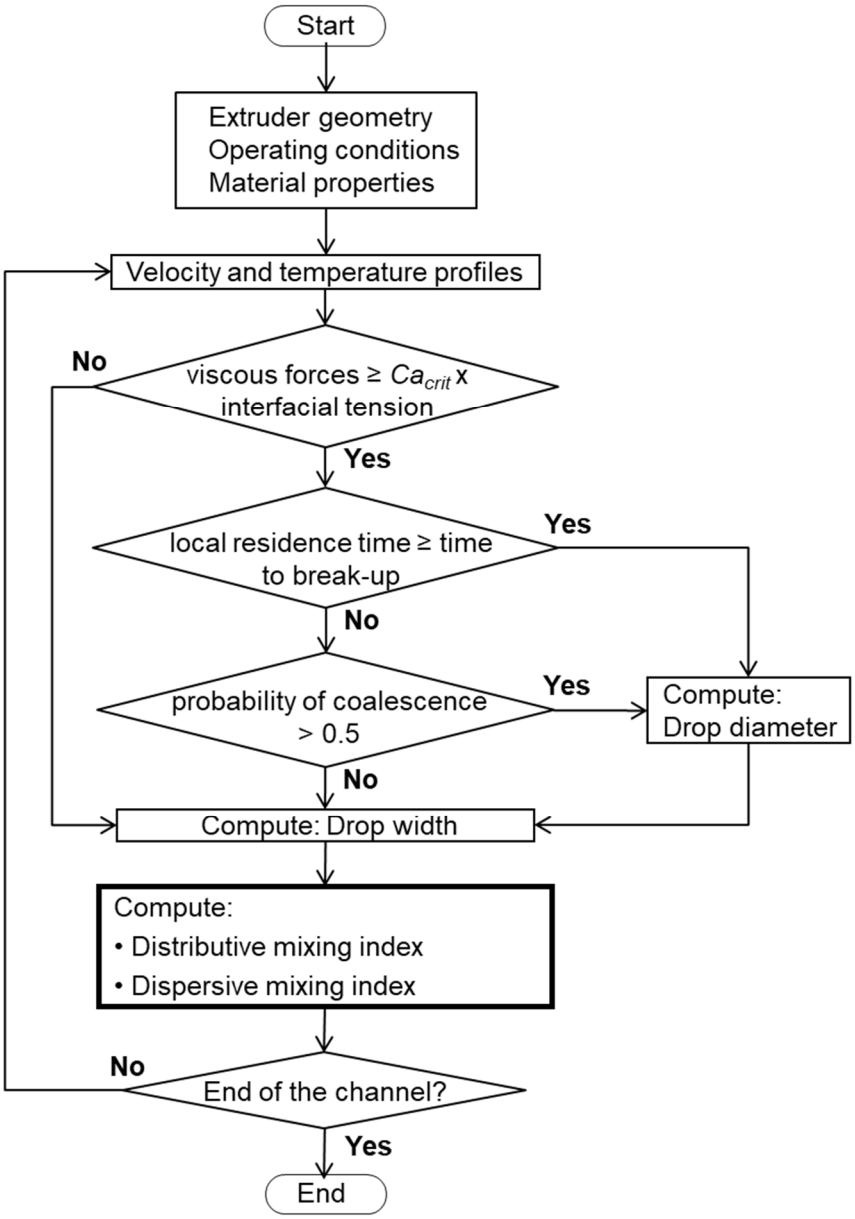


Figure 4 - Algorithm for predicting morphology evolution and mixing for a liquid–liquid system.

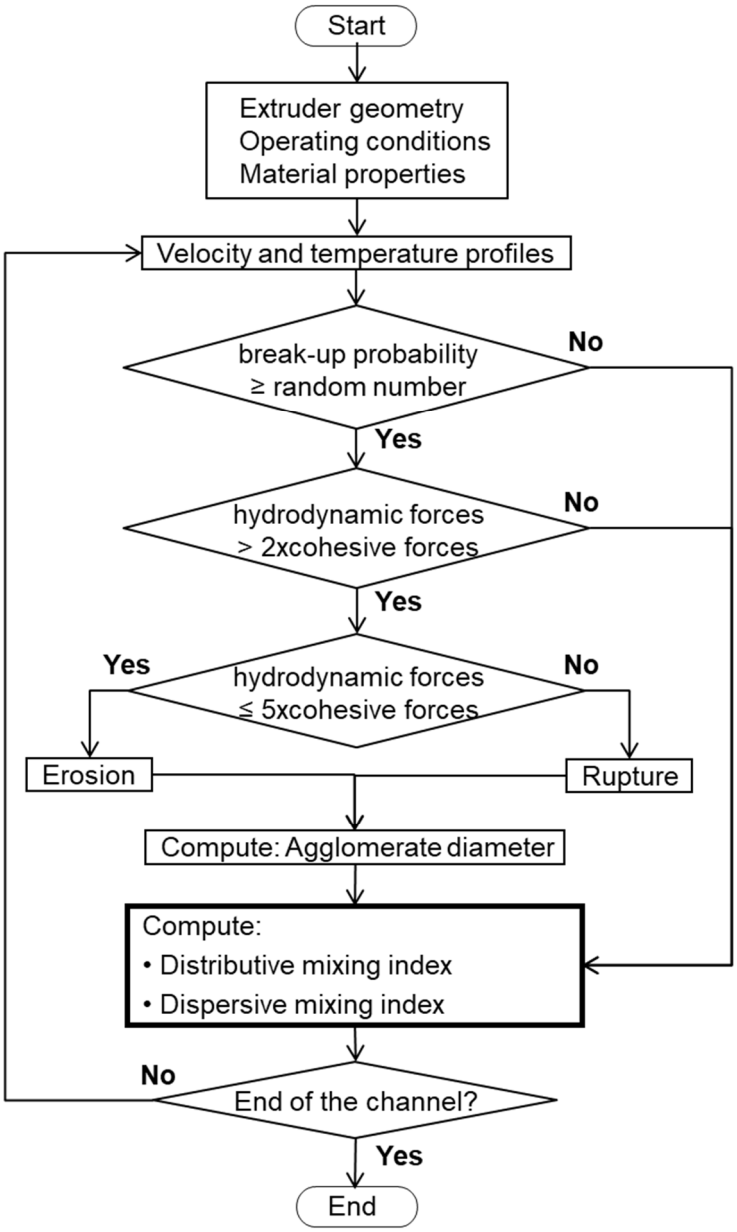


Figure 5 - Algorithm for predicting morphology evolution and mixing for a liquid–liquid system

## 4. Selected Results

This section presents a few illustrative results obtained when applying the algorithms presented so far to specific material/extruder/operating conditions combinations.

Figure 6 portrays the axial evolution of pressure and of the relative presence of solids (in terms of the ratio between the solids width, *X* and the channel width, *W*). X decreases progressively downstream, hence only a portion of the channel downstream works fully filled with melt. As a radar plot, Figure 7 shows the influence of screw speed on mass output, mechanical power consumption, axial length of screw required for melting, average melt temperature, degree of

distributive mixing (WATS) and maximum viscous dissipation (ratio of maximum melt temperature to barrel temperature) for a specific set of imput conditions. An increase in screw speed produces an increase in mass output, but at the cost of additional mechanical power consumption, greater viscous dissipation (and melt temperatures) and lower mixing quality (generally, WATS deteriorates as the screw speed increases, since a shorter channel section becomes available for mixing due to the gradual lower melting rates and shorter residence times).

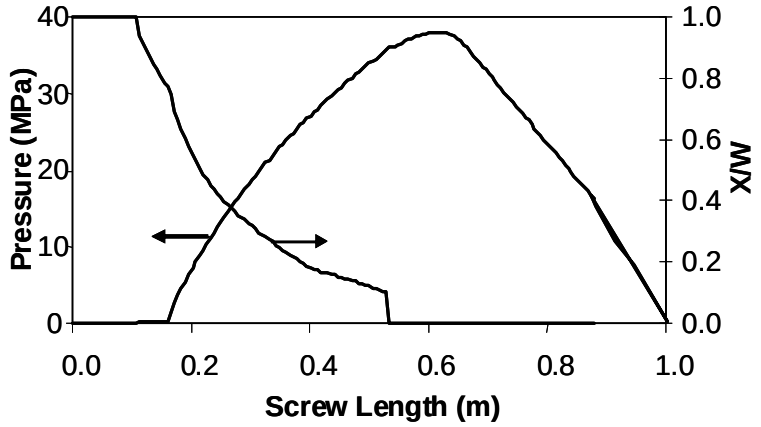


Figure 6- Axial profiles of pressure and relative presence of solids (at 60 rpm).

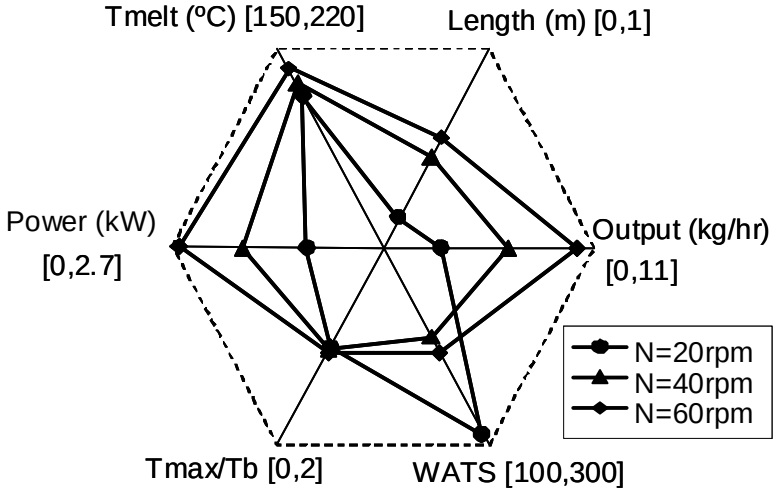


Figure 7- Influence of screw speed on various process parameters for a specific material and extruder geometry.

Figure 8 concerns the evolution of the morphology of a liquid-liquid system (typically, an immiscible polymer blend), for different values of the viscosity ratio *p* of the components. The graph on top represents the development of the average drop size, d, together with the corresponding standard deviation, whereas the chart at the bottom shows the progress of the average drop length, L. Melting extends approximately from L/D = 7 to L/D = 18, i.e., it contributes significantly to dispersion. As observed by Grace [23], as the ratio p decreases, drop break-up occurs under higher shear rates, but the time for drop break-up also decreases and dispersion becomes more effective. This is confirmed in Fig. 8 for values of p of 1 and $10^{-2}$. For lower values of p, the time for drop break-up tends to zero, but dispersion becomes less important because it requires higher shear rates than those attained under the operating conditions considered.

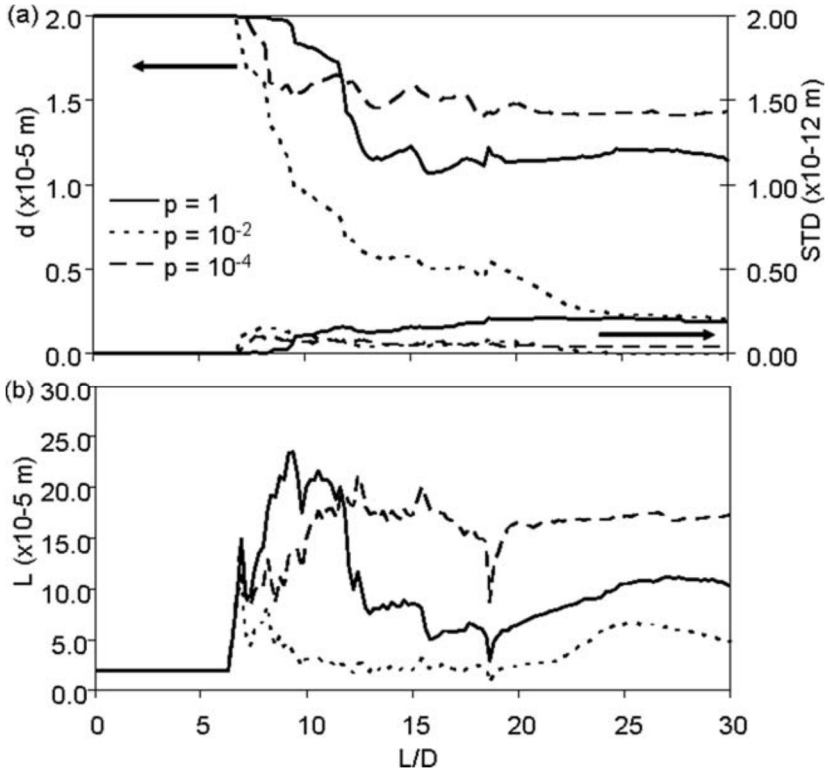


FIG. 8. Effect of the viscosity ratio on the average drop diameter (a) and drop length (b) of the minor phase.

Figure 9 demonstrates the dynamics of the progress of the dimensions of solid particles suspended in a melt for a particular solids-liquid system. All fluid elements follow helical patterns along the channel; each of the 4 images correspond to the flow times indicated. The (unwrapped) rectangular channel corresponds to the metering zone of a screw, the flow developing vertically upwards. At the inlet, 1000 agglomerates with an uniform size of 100μm

are assumed as regularly distributed. The progressive conversion of these agglomerates into aggregates and then into primary particles is evident. At short residence times, the primary particles should be formed from the erosion of bigger particles. At the outlet, 20% of the agglomerates survive, and a range of particle sizes is present (aggregates are about 50μm in diameter, primary particles between 1 and 4 μm) [28]. This type of predictions has a physical equivalence, despite the difficulty in performing an experimental validation [28].

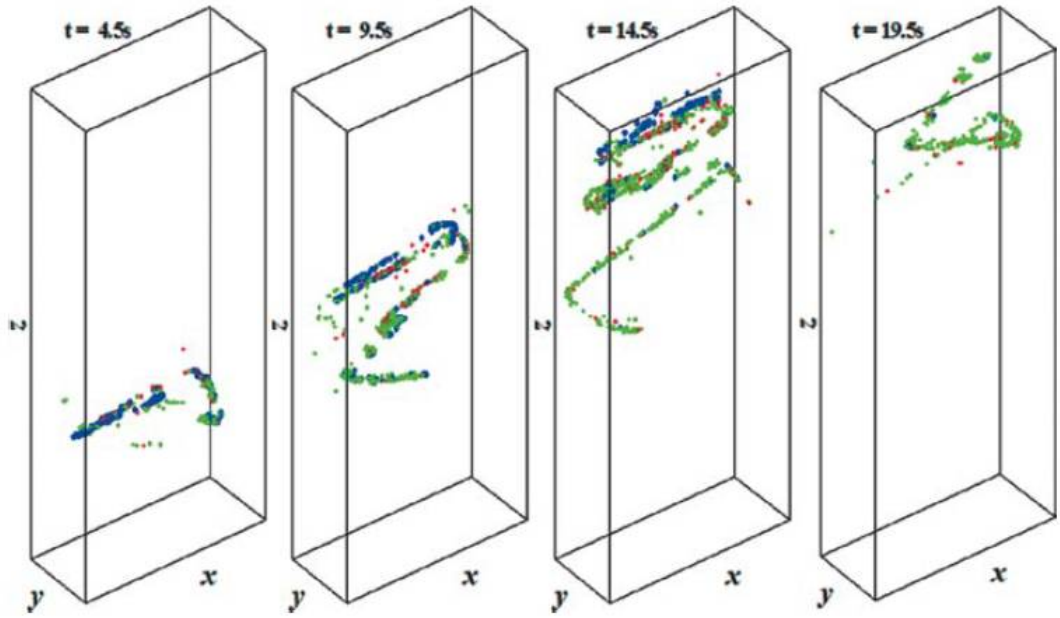


Figure 9 - Flow (vertically upwards) in the metering zone of the (unwrapped) screw; during the helical flow the parent agglomerates (blue) are progressively broken into aggregates (green) and primary particles (red).

Figure 10 displays examples of the evolution along the screw of the global mixing indices for two different screw speeds (50 and 200 rpm). As observed above for liquid-liquid systems, the melting stage can have a significant contribution to mixing (albeit this being often ignored in the calculations published in the literature). This role should be expected, given the relatively high shearing rates developing in melt films (surrounding the solid plug) and melt pool (particularly towards the end of the compression zone of the screw). As the screw speed increases, the melting zone usually becomes longer, thus further increasing its importance to mixing.

Distribution and dispersion continue along the melt conveying zone. In this particular example, the dispersion of the liquid-liquid system advances gradually, as breakup requires not only

enough shear stresses, but also sufficient residence time. In the case of the solid-liquid system, dispersion by erosion seems to be followed by the distribution of the particles just generated.

The relative unsteadiness of the curves in the melting stage, as well as the eventual decrease of the actual value of a mixing index along the screw axis, are due to the insertion of new suspended material during melting of the matrix, as part of the calculation algorithms presented in the preceding sections. Please note that upon melting of the matrix, the average size of the particles/droplets results from the balance between their dispersion and the number and size of the new entities injected into the system. As these new entities are not deformed and are assumed as uniformly distributed in the melt, they also affect negatively the local distribution.

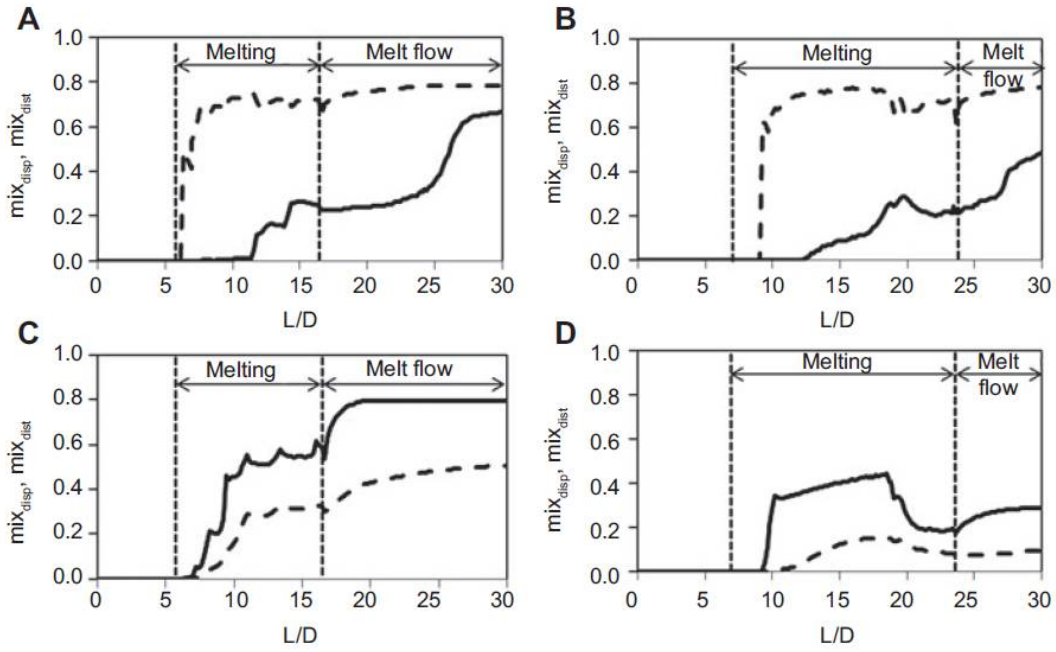


Figure 10 – Axial evolution of distributive (broken lines) and dispersive (solid lines) global mixing indices along a single screw extruder. (A) Liquid-liquid system, screw rotating at 50 rpm; (B) liquid-liquid system, screw rotating at 200 rpm; (C) solid-liquid system, screw rotating at 50 rpm; (D) solid-liquid system, screw rotating at 200 rpm.

## 5. Conclusions

Single screw extruders are one of the most important processing equipments used by the industrial plastics sector. They accept the raw material as powder or pellets, melt it and generate the pressure necessary for a continuous flow through the shaping die. The performance of these machines depends on their geometry/construction, material properties and operating conditions. However, the interrelationship between these is far from obvious. Therefore, the

design of improved screws, or the selection of the appropriate operating conditions for the successful manufacture of a given product from a specific polymer system, will greatly benefit from the support of precise process modelling tools.

It is currently possible to couple descriptions of flow and heat transfer along the screw to models describing the development of the morphlogy of complex polymer systems, such as polymer blends and composites. Thus, processors can now acquire a detailed picture of the process for a given set of input conditions and thus make more informed decisions. Also, these routines can be used for processing optimization, which will be dealt with in a separate chapter.

## 6. References


[1] Z. Tadmor, I. Klein, *Engineering Principles of Plasticating Extrusion*, Van Nostrand Reinhold, New York (1970)

[2] C C Chung, *Extrusion of Polymers Theory and Practice*, 2nd ed., Hanser Publishers, Munich (2000)

[3] C. Rauwendaal, *Polymer Extrusion*,5th ed. Hanser Publishers, Munich (2014)

[4] M.J. Stevens, J.A. Covas, *Extruder Principles and Operation*, 2nd ed., Chapman & Hall, London (1995).

[5] D G Baird, D I Collias, *Polymer Processing Principles and Design*,2nd ed., John Wiley & Sons, Inc., Hoboken, New Jersey (2014)

[6] Z Tadmor, C Gogos, *Principles of Polymer Processing*, 2nd ed., Wiley- Interscience, John Wiley & Sons, Inc., Hoboken, New Jersey (2006)

[7] Michelangelli, O. P., Gaspar-Cunha, A., & Covas, J. A. (2014). The influence of pellet-barrel friction on the granular transport in a single screw extruder. *Powder Technology*, *264*(9), 401–408.

[8] Michelangelli, O., Yamanoi, M., Gaspar-Cunha, A., & Covas, J. A. (2011). Modelling pellet flow in single extrusion with DEM. *Journal of Process Mechanical Engineering*, *225*(Part E), 255–268.

[9] D.M. Walker, *An Approximate Theory for Pressures and Arching in Hoppers*, Chem. Eng. Sci., 21, pp. 975-997 (1966).

[10] E. Broyer, Z. Tadmor, *Solids Conveying in Screw Extruders – Part I: A modified Isothermal Model*, Polym. Eng. Sci., 12, pp. 12-24 (1972).

[11] Z. Tadmor, E. Broyer, *Solids Conveying in Screw Extruders – Part II: Non Isothermal Model*, Polym. Eng. Sci., 12, pp. 378-386 (1972).

[12] H. Darnell, E.A.J. Mol, *Solids Conveying in Extruders*, SPE J., 12, pp. 20-29 (1956).

[13] L. Kacir, Z. Tadmor, *Solids Conveying in Screw Extruders – Part III: The Delay Zone*, Polym. Eng. Sci., 12, pp. 387-395 (1972).

[14] J-F Agassant, P Avenas, P J. Carreau, B Vergnes, M Vincent, *Polymer Processing Principles and Modelling*, 2nd ed., Carl Hanser Verlag, Munchen, Germany (2017)

[15] Gaspar-Cunha, A. (2009). *Modelling and Optimisation of Single Screw Extrusion Using Multi-Objective Evolutionary Algorithms* (1st ed.). Koln, Germany: Lambert Academic Publishing.

[16] B.H. Maddock, *A Visual Analysis of Flow and Mixing in Extruder*, Soc. Plast. Engs. J., 15, pp. 383-394 (1959).

[17] J.T. Lindt, B. Elbirli, *Effect of the Cross-Channel Flow on the Melting Performance of a Single-Screw Extruder*, Polym. Eng. Sci, 25, pp. 412-418 (1985).

[18] B. Elbirli, J.T. Lindt, S.R. Gottgetreu, S.M. Baba, *Mathematical Modelling of Melting of Polymers in a Single-Screw Extruder*, Polym. Eng. Sci., 24, pp. 988- 999 (1984).

[19] Domingues, N., Gaspar-Cunha, A., & Covas, J. A. (2010). Estimation of the morphology development of immiscible liquid–liquid systems during single screw extrusion. *Polymer Engineering and Science*, *50*(11), 2194–2204.

[20] ANSYS, Inc, www.ansys.com

[21] I Manas-Zloczower (ed.) *Mixing and Compounding of Polymers*, 2nd ed., Hanser Publishers, Munich, 521 (2009).

[22] Domingues, N., Gaspar-Cunha, A., & Covas, J. A. (2012). A Quantitative Approach to Assess the Mixing Ability of Single Screw Extruders for Polymer Extrusion. *Journal of Polymer Engineering*, *32*(2), 81–94.

[23] H.P. Grace, *Dispersion phenomena in high viscosity immiscible fluid systems and application of static mixers as dispersion devices in such systems*, Chem. Eng. Commun., 14, 225 (1982).

[24] P G Lafleur, B Vergnes, *Polymer Extrusion*, John Wiley & Sons, Inc, Hoboken, USA (2014)

[25] Y.M. Stegeman, *Time Dependent Behavior of Droplets in Elongational Flows*, PhD Thesis, Tech. Univ. Eindhoven, The Netherlands (2002).

[26] L. Delamare, B. Vergnes, *Computation of the morphological changes of a polymer blend along a twin-screw extruder*, Polym. Eng. Sci., 36, 1685 (1996).

[27] Scurati, A., Feke, D.L., Manas-Zloczower, I., *Analysis of the Kinetics of Agglomerate Erosion in Simples Shear Flows*, Chem. Eng. Sci., 60, p. 6564-6573 (2005)

[28] Domingues, N., Gaspar-Cunha, A., Covas, J. A., Camesasca, M., Kaufman, M., & Manas-Zloczower, I. (2010). *Dynamics of Filler Size and Spatial Distribution in a Plasticating Single Screw Extruder – Modeling and Experimental Observations*. *International Polymer Processing*, *25*(3), 188–198.

[29] G. Pinto, Z. Tadmor, *Mixing and Residence Time Distribution in Melt Screw Extruders*, Polym. Eng. Sci., 10, pp. 279-288 (1970).